Analog Complex Wavelet Filters

Sandro A. P. Haddad†, Joël M. H. Karel‡, Ralf L. M. Peeters‡,
Ronald L. Westra‡ and Wouter A. Serdijn†

†Electronics Research Laboratory, Faculty of Electrical Engineering, Mathematics and Computer Science,
Delft University of Technology, Mekelweg 4, 2628 CD Delft, The Netherlands
Email:[s.haddad, w.a.serdijn]@ewi.tudelft.nl
‡Department of Mathematics, University of Maastricht P.O.Box 616, 6200 MD, Maastricht, The Netherlands
Email: [joel.karel,ralf.peeters,westra]@math.unimaas.nl

***Abstract*— This paper presents an analog implementation of the complex wavelet transform using both the complex first order system (CFOS) and the Padé approximation. The complex wavelet filter design is based on the combination of the real and the imaginary state-space descriptions that implement the respective transfer functions. In other words, a complex filter is implemented by an ordinary state-space structure for the real part and an extra C matrix for the imaginary part. Several complex wavelets, such as Gabor, Gaussian and Morlet complex wavelets, are obtained and simulations demonstrate excellent approximations to the ideal wavelets.**

I. Introduction

Complex wavelets provide more detailed information in transient signal detection than real-valued wavelets. Often the wavelet transform of a real signal with complex wavelet is plotted in modulus-phase form, rather than in real and imaginary representation. In the complex wavelet transform analysis, the modulus maxima and the phase crossings point out the locations of sharp signal transitions. Nevertheless, the phase information reveals isolated singularities in a signal more accurately than does the modulus [1]. Also, using the phase information, different kinds of transition points of the analyzed signal, i.e. local maxima and inflection points, can be distinguished. For instance, using the first complex Gaussian wavelet ($cgau1$), the $-\pi$ to $+\pi$ phase crossings correspond to the inflection points, whereas the phase transition between $\pm\pi$ to 0 is associated with the local maxima points (peaks), as one can see in Fig.1.

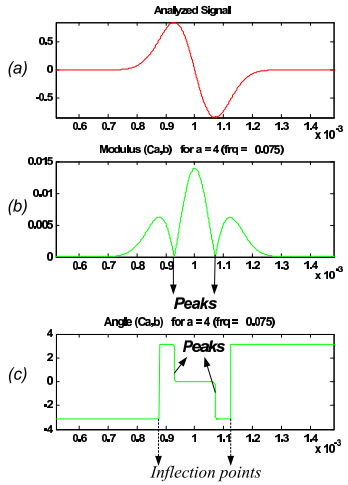

Fig. 1. Complex wavelet transform using cgau1 (a) Input signal (b) Wavelet transform coefficient line ($a = 4$) - Modulus (c) Wavelet transform coefficient line ($a = 4$) - Phase

Section II treats the complex wavelet bases and deals with the computation of a transfer function which describes a certain wavelet base that can be implemented as an analog filter. Section III describes the circuit designs. Some results provided by simulations are given in Section IV. Finally, Section V presents the conclusions.

II. Complex Wavelet Filters

A. Complex wavelet bases

One example of a complex wavelet function is the Gabor wavelet. The Gabor wavelet is obtained from a complex Gaussian function (complex exponential windowed by a Gaussian function) as basic functions [2], as described by

$$\psi(t) = C \cdot e^{-j\omega t} e^{-t^2} = Ccos(\omega t)e^{-t^2} - jCsin(\omega t)e^{-t^2} \quad (1)$$

where $e^{-j\omega t}e^{-t^2}$ is the complex Gaussian function and C is a normalizing constant. From the Gabor wavelet one can derive some complex wavelet families, e.g. the complex Gaussian and the complex Morlet. The complex Morlet wavelet is obtained by simply applying $\omega = \pi\sqrt{\frac{2}{ln2}} \simeq 5.3364$ [3] in Eq.1.

The complex Gaussian wavelet family is defined from the derivatives of the Gabor wavelet [2] and is given by

$$\psi_n(t) = C_n \cdot \frac{d^n}{dt^n}(e^{-j\omega t}e^{-t^2}) \quad (2)$$

where n denotes the order, $\frac{d}{dt}$ is the symbolic derivative and C is a normalizing constant, which depends of n.

The wavelet used in this paper is the complex Gabor wavelet, from which we can derive other complex wavelets. The modulus, the real and imaginary parts and the phase of the complex Gabor wavelet for $\omega = 2$ are given in Fig.2.

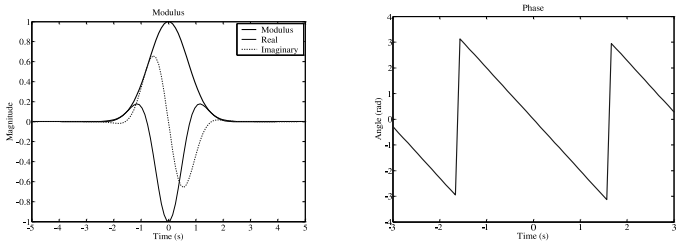

(a) (b)

Fig. 2. Complex Gabor Wavelet (a) Modulus (b) Phase

B. Complex First Order filters

In order to implement the complex Gabor wavelet filter, we first propose an analog filter based on the Complex First Order Systems (CFOS) [4]. A CFOS is defined by the following set of equations

$$\dot{x}(t) = -(\sigma + j\omega)x(t) + (c_{re} + jc_{imag})u(t) \quad (3)$$

$$x(t) = x_{re}(t) + jx_{imag}(t) \quad (4)$$

where u is the input signal assumed to be real, x is the state variable assumed to be complex, σ, ω, c_{re} and c_{imag} are system parameters assumed also to be real. Without loss of generality we will assume c_{re} and c_{imag} to be equal to 1. One can map this first order transfer function onto a state space description. The general expression of the transfer function corresponding to a state space description is

$$H(s) = C \cdot (sI - A)^{-1} \cdot B + D \quad (5)$$

The entries of the matrices A, B, C and D are derived directly from the coefficients of the transfer function. The poles of the transfer function are the eigenvalues of A. In other words, the denominator of the transfer function is given by the determinant of $sI - A$, where I is the identity matrix. The zeros of the filter are constituted from the contents of all four system matrices. Considering $D = 0$, and applying $C \cdot adj(sI - A) \cdot B$, where adj compute the adjoint of the respective matrix, we can obtain a possible state space description of H_{re} and H_{imag} given by

$$A_{re,im} = \begin{bmatrix} -\sigma & \omega \\ -\omega & -\sigma \end{bmatrix} \quad B_{re,im} = \begin{bmatrix} 0 \\ 1 \end{bmatrix}$$

$$C_{re} = \begin{bmatrix} 0 & 1 \end{bmatrix} \quad C_{im} = \begin{bmatrix} 1 & 0 \end{bmatrix} \quad (6)$$

Notice that the state space descriptions differ only by the C matrices. Then, we can represent the CFOS using the following block diagram, given in Fig.3

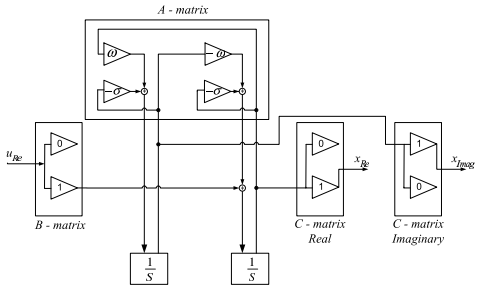

Fig. 3. Complex First Order System block diagram using state-space representation

An imaginary input can be added by just including another B stage. From this block diagram, one can easily derive the common CFOS cross-coupled representation in Fig.4

The starting point of the Gabor wavelet design using CFOS is the definition of the number of stages which defines the appropriate Gaussian envelope to set the width of the wavelet [4]. Subsequently, once the Gaussian envelope has been defined, the real and the imaginary impulse responses are obtained. Applying Eq. 3 and Eq. 4, the complex impulse response of $n + 1$ CFOS stages is given by

$$h(t) = (c_{re} + jc_{imag})^{n+1} \frac{t^n}{n!} e^{-(\sigma+j\omega)t} U_{-1}(t) \quad (7)$$

From Eq.7 one easily calculates the general transfer function of the $n + 1$ CFOS system for the real and the imaginary outputs, which

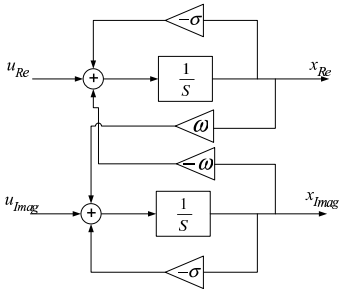

Fig. 4. Complex First Order System block diagram

are given as follows

$$H_{re}(n) = \frac{(s+\sigma) \cdot H_{re}(n-1) - \omega \cdot H_{imag}(n-1)}{\left((s+\sigma)^2 + \omega^2\right)^{n-1}} \quad (8)$$

$$H_{imag}(n) = \frac{(s+\sigma) \cdot H_{imag}(n-1) + \omega \cdot H_{re}(n-1)}{\left((s+\sigma)^2 + \omega^2\right)^{n-1}} \quad (9)$$

with

$$H_{re}(1) = \frac{(s+\sigma)}{(s+\sigma)^2 + \omega^2} \quad (10)$$

$$H_{imag}(1) = \frac{\omega}{(s+\sigma)^2 + \omega^2} \quad (11)$$

which correspond to the transfer function of the first order complex filter in Fig.3. Choosing the right values for σ and ω, we can obtain the imaginary and the real part of the complex Gabor, respectively, as one can see in Fig.5 for different numbers of stages.

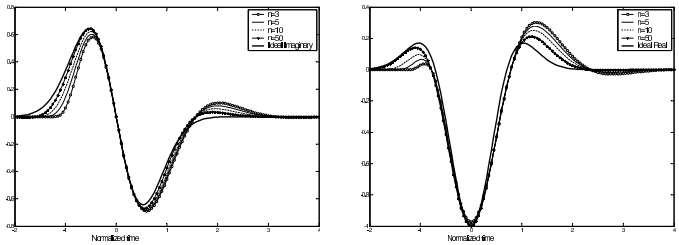

(a) (b)

Fig. 5. Complex Gabor Impulse response (a) Imaginary output (b) Real output

It must be noted that the Complex Morlet Wavelet can also be approximated in a similar manner. Again, we need to choose the right value for ω in order to have the appropriate frequency component for the Morlet wavelet.

C. Padé Approximation in Laplace domain

In the previous section, an analog complex wavelet transform filter was proposed, of which the impulse responses are approximated complex Gaussian window functions. This complex wavelet filter, subsequently, was implemented with CFOS technique. However, a more general procedure based on the Padé approximant to obtain various types of wavelet bases was presented in [5]. Moreover, the Padé method proves to be more successful than the method using

CFOS for a filter of the same order which will be shown in this section.

Just like the Taylor expression, the Padé approximation is an approximation that concentrates around one point of the function that needs to be approximated (i.e. the impulse response $h(t)$) [6]. In the Padé approximation, the coefficients of the approximating rational expression are computed from the Taylor coefficients in the Laplace domain of the original function. The reason to apply the Padé approximation to the Laplace transform of $h(t)$ is, that it immediately yields a rational expression which is suitable for implementation. A Padé approximation of function $F(s)$ is given by

$$\hat{F}(s) = \frac{P(s)}{Q(s)} = \frac{p_0 + p_1 s + \ldots + p_m s^m}{q_0 + q_1 s + \ldots + q_n s^n} \tag{12}$$

where $\hat{F}(s)$ is the Taylor series truncated around some point, e.g. $s = 0$ and $q_n = 1$ for normalization. If the approximating rational function has a numerator of order *m* and a denominator of order *n*, the original function can be approximated up to order $m + n$. The computation of the coefficients of $P(s)$ and $Q(s)$ has already been described in [5], [6].

One can first apply the Padé technique to approximate the Gaussian envelope. We apply a $[2/5]$ Padé approximation, i.e. $m = 2$ and $n = 5$, which yields an approximation of order $k = 7$ of the Taylor series expansion. The transfer function resulting from this approximation is given by

$$H_{gaus}(s) = \frac{5.7s^2 - 18.2s + 92.416}{s^5 + 8.3s^4 + 33s^3 + 74.8s^2 + 94.5s + 52.3} \tag{13}$$

In order to obtain the transfer function of the real and the imaginary parts of the Gabor function in Eq.1 one can easily apply

$$H_{Gabor}(s) = \frac{s}{s^2 + \omega^2} * H_{gaus}(s) - j\frac{\omega}{s^2 + \omega^2} * H_{gaus}(s) \tag{14}$$

where the asterisk $*$ is the symbol for convolution and $\frac{s}{s^2+\omega^2}$ and $\frac{\omega}{s^2+\omega^2}$ are the Laplace transforms of $cos(\omega t)$ and $sin(\omega t)$, respectively. Notice that both transfer functions are related by

$$H_{\mathrm{Real}}(s) = -\frac{s}{\omega} * H_{\mathrm{Imag}}(s) \tag{15}$$

From Eq.15, one can verify that the poles of the real and the imaginary transfer function are the same, only differing in the zeros. Therefore, we can implement both transfer functions by changing only the C-matrix of the state-space representation, as shown in Fig.6.

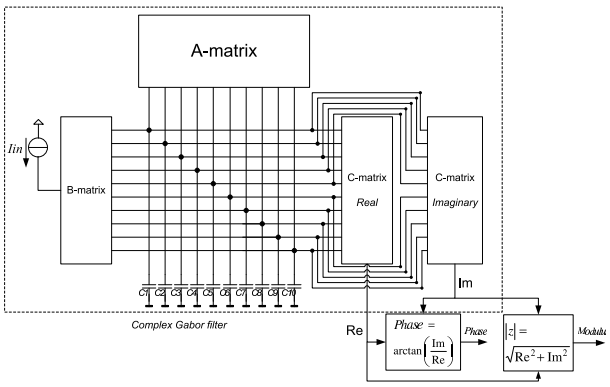

Fig. 6. Block diagram of the Complex Wavelet system

Using the procedure described in Eq.14, yields tenth order transfer functions with 7 zeros. Its corresponding impulse responses are given in Fig.7.

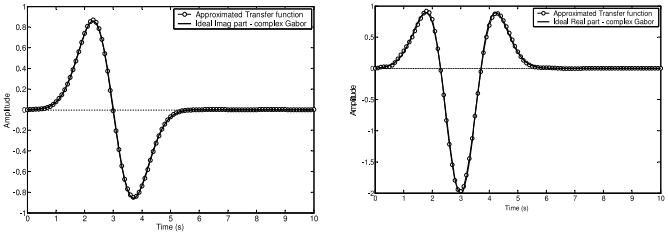

(a) (b)

Fig. 7. Complex Gabor Impulse response approximation (a) Imaginary output (b) Real output

In order to compare the Padé approximation with the approximation using CFOS one can verify the associated Mean-Square Error for both approximation. The results obtained varying the order of the filter are illustrated in Table.I, where the real and the imaginary parts of the complex Gabor wavelet have been approximated, respectively.

order	CFOS		Padé	
n	Real	Imaginary	Real	Imaginary
3	0.0444	0.0513	0.0899	0.0927
4	0.0382	0.0380	0.0817	0.0468
5	0.0339	0.0302	0.0454	0.0185
6	0.0308	0.0251	0.0178	6.05e-3
7	0.0284	0.0216	7.75e-3	1.01e-3
8	0.0265	0.0190	2.30e-3	0.040e-3
9	0.0250	0.0170	0.74e-3	0.033e-3
10	0.0238	0.0154	0.13e-3	0.020e-3

TABLE I
ORDER OF THE FILTER VERSUS MEAN-SQUARE ERROR FOR CFOS AND PADÉ APPROXIMATION

As seen from the Mean-Square Error comparison for $n > 5$, the Padé method yields a much better approximation than the method using CFOS for a filter of the same order. Finally, by only changing the numerator coefficients of the Eq.14 (i.e. the zeros), we can obtain the complex Gaussian and the complex Morlet wavelets.

III. CIRCUIT DESIGN

A. Filter design

The filter design that follows is based on an orthonormal ladder structure , which presents a good behavior with respect to sensitivity and dynamic range [5], with log-domain integrators as the main building blocks. A simple bipolar multiple-input low-power log-domain integrator [7] will be used as the basic building block for the implementation of the tenth order state space equations of the Gabor wavelet filter described in the previous section. This log-domain integrator is shown in Fig.8.

B. Modulus stage

The static translinear principle can be applied to the implementation of the required nonlinear transfer functions of the modulus and arctangent stages. First, the required modulus function $|z| =$

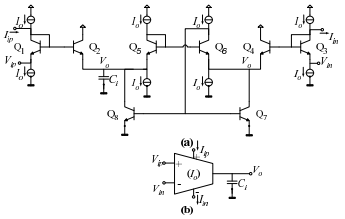

Fig. 8. (a) The multiple-input low power log-domain integrator, and (b) its symbol [7]

$\sqrt{\mathrm{Re}^2 + \mathrm{Im}^2}$ is realized with the circuit in Fig.9(a) [8]. The translinear loops in the circuit consist of transistors Q_1, Q_7, Q_8 and Q_4 and Q_6, Q_{11}, Q_{10} and Q_4, implementing

$$2(I_o - \mathrm{Re})(I_o + \mathrm{Re}) = (\sqrt{2}I_o - z)(\sqrt{2}I_o + z + p)$$
$$2(I_o - \mathrm{Im})(I_o + \mathrm{Im}) = (\sqrt{2}I_o - z)(\sqrt{2}I_o + z - p) \qquad (16)$$

where I_o is the bias current and p is a coupling parameter equal to $\frac{2Re^2 - z^2}{z - \sqrt{2}I_o}$. Notice that both variables, Re and Im, are bipolar quantities.

C. Phase information - Arctangent stage

From the complex waveforms shown in Fig.7, we can now obtain the phase information by simply applying the arctangent to the ratio between the imaginary and the real outputs. This operation can be approximated using the translinear principle as [8]

$$Phase = \frac{Im}{0.63Re + \sqrt{0.88Re^2 + Im^2}} \simeq \frac{2}{\pi} arctan(\frac{Im}{Re}) \qquad (17)$$

where the square root term is provided by the modulus circuit in previous section. The division operation can easily be implemented using the factorization $z = \frac{x}{y} \Rightarrow \frac{Io+z}{Io-z} = \frac{y+x}{y-x}$ [8] and the schematic is given in Fig.9(b) [9].

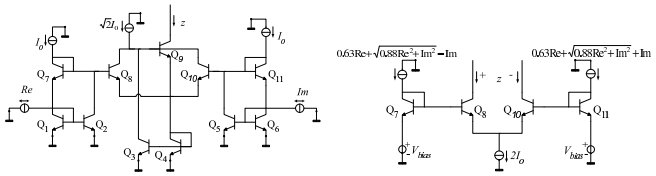

(a) (b)

Fig. 9. (a) Modulus (Vector magnitude) circuit [8] (b) Divider circuit for the Arctangent stage [9]

IV. Simulations results

To validate the circuit principle, we have simulated the filter, the modulus stage and the phase stage using models of IBM's $0.18\mu m$ BiCMOS IC technology. The filter has been designed to operate from a 1.2V supply and a 100pF total capacitance. Fig.10 shows the impulse response of the real and imaginary outputs of the wavelet filter. The excellent approximation of the complex Gabor wavelet can be compared with the ideal Gabor function to confirm the performance of the filter. Finally, Fig.11 shows the modulus stage and phase stage outputs, which are close to the ideal cases for the complex Gabor wavelet in Fig.2.

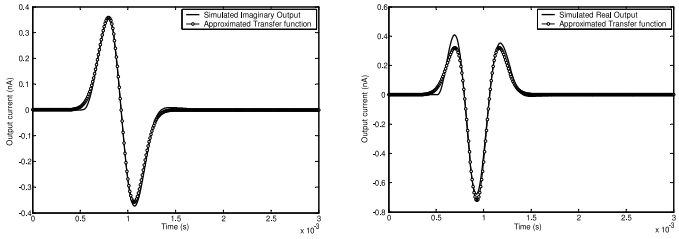

(a) (b)

Fig. 10. Simulated impulse responses of the complex Gabor wavelet filter (a) Imaginary output (b) Real output

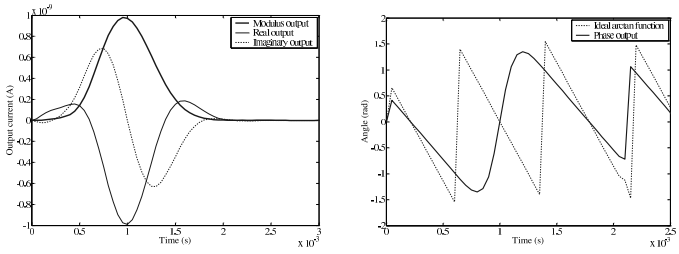

(a) (b)

Fig. 11. Simulated complex Gabor wavelet filter (a) Modulus and (b) Phase responses

V. Conclusions

An analog implementation of the complex wavelet transform was presented. The procedure was based on either CFOS or the Padé approximation . The complex wavelet filter design was derived from the combination of the real and the imaginary state-space descriptions. By this, we were able to implement a complex filter, i.e. both real and imaginary transfer functions, with just an extra C matrix into an ordinary state-space structure. Several complex wavelets have been obtained and simulations demonstrated excellent approximations to the ideal wavelets.

References

[1] M. Unser and A. Aldroubi, "A review of wavelets in biomedical applications," *Proceeding of the IEEE*, vol. 84, no. 4, April 1996.

[2] S.Mallat, *A Wavelet Tour of Signal Processing*, Academic Press, 2001.

[3] I. Daubechies, *Ten Lectures on Wavelets*, Society for Industrial and Applied Mathematics, Philadelphia, 1992.

[4] H. Kamada and N. Aoshima, "Analog gabor transform filter with complex first order system," *in Proc. SICE*, pp. 925–930, 1997.

[5] S. A. P. Haddad, S. Bagga, and W. A. Serdijn, "Log-domain wavelet bases," in *Proceedings IEEE International Symposium Circuits and Systems*, May 2004, vol. 1, pp. 1100–3.

[6] G. A. Baker Jr., *Essentials of Pade Approximants*, Academic Press, New York, 1975.

[7] M. N. El-Gamal and G. W. Roberts, "A 1.2v npn-only integrator for log-domain filtering," *IEEE Transactions on Circuits and Systems - II: Analog and Digital Signal Processing*, vol. 49, no. 4, pp. 257–265, April 2002.

[8] E. Seevinck, *Analysis and Synthesis of Translinear Integrated Circuits*, Elsevier, The Netherlands, 1988.

[9] C. Toumazou, F. J. Lidgey, and D. G. Haigh, *Analogue IC design: the current-mode approach*, IEE circuits and systems series 2, United Kingdom, 1990.